# Mesoporous Silica Molecular Sieves Prepared by Ionic and Neutral Surfactant Templating: A Comparison of Physical Properties

Peter T. Tanev and Thomas J. Pinnavaia*

*Department of Chemistry and Center for Fundamental Materials Research, Michigan State University, East Lansing, Michigan 48824-1322*

*Received November 16, 1995. Revised Manuscript Received February 28, 1996*[⊗]

A series of mesoporous MCM-41 and HMS silica molecular sieves have been prepared by electrostatic and neutral assembly pathways, respectively, and their properties have been compared by a variety of physical techniques. Direct $S^+I^-$ charge matching between cationic quaternary ammonium ion surfactants ($S^+$) and the anionic silicate precursors ($I^-$) affords long-range hexagonal structures under hydrothermal synthesis conditions (100 °C), but the long-range order is greatly reduced when the synthesis is conducted at ambient temperature. Conversely, owing to weaker assembly forces, counterion-mediated $S^+X^-I^+$ and neutral $S^0I^0$ pathways (where $X^-$ is halide and $S^0$ is a primary amine) provide calcined products with the best long-range order when the syntheses are conducted at ambient temperature. In general, MCM-41 silicas formed by electrostatic $S^+I^-$ or $S^+X^-I^+$ assembly exhibit greater long-range order than the HMS analogues prepared by the $S^0I^0$ assembly. However, the framework-confined pore structures, though dependent on the size of the surfactant, remain uniform, regardless of the fidelity of the long-range hexagonal order. As-synthesized neutral HMS silicas are much more extensively cross-linked than the as-synthesized charged frameworks of MCM-41 analogues, as judged by the $^{29}$Si MAS NMR $Q^4/Q^3$ $Si(O-Si)_{4-x}$ connectivity ratios. The neutral and extensively cross-linked character of HMS frameworks allows for the efficient and environmentally benign recovery of the template by solvent extraction. In contrast, electrostatically templated MCM-41 derivatives require proton ion exchange or calcination for the complete removal of template from the framework pores. Also, relative to the $S^+I^-$ and $S^+X^-I^+$ templated derivatives, HMS mesostructures generally possess thicker framework walls, superior thermal stability upon calcination in air, and a smaller crystallite size, which affords complementary textural mesoporosity for improved access to the framework-confined mesopores.

## Introduction

In 1992 scientists at Mobil Oil Research and Development announced the direct synthesis of the first broad family of mesoporous molecular sieves (denoted M41S) using cationic surfactants to assemble silicate anions from solution.[1,2] Three members of the M41S family of materials were distinguished: hexagonal MCM-41, cubic MCM-48, and a lamellar MCM-50 silica phase. The originally proposed mechanism for MCM-41 formation involved strong electrostatic interactions and charge matching between *micellar assemblies* of quaternary ammonium cations ($S^+$), as structure-directing agents and anionic silicate oligomer species ($I^-$).[1]

Also, Kuroda et al. reported the surfactant directed rearrangement of a single-sheet silicate, kanemite ($NaHSi_2O_5\cdot 3H_2O$), into a long-range ordered hexagonal surfactant−inorganic complex.[3] The driving force for this framework transformation process was provided by the electrostatic interactions between micellar assemblies of intercalated quaternary ammonium surfactants ($S^+$) and the negatively charged layered host ($I^-$). The cooperative character of the electrostatic $S^+I^-$ assembly mechanism has been verified by the subsequent work of Stucky et al. and Davis et al.[4−6]

The electrostatic assembly approach has been extended to other mesostructured compositions by implementation of four complementary synthesis routes.[7] The primary pathway involved the direct co-condensation of anionic inorganic species ($I^-$) with a cationic surfactant ($S^+$) affording assembled ion pairs of a type $S^+I^-$, the original synthesis of MCM-41 silicas being the seminal example.[1,2] In the second pathway, the charge-reversed case, an anionic template ($S^-$) was used to direct the

---

[⊗] Abstract published in *Advance ACS Abstracts,* July 15, 1996.

(1) Beck, J. S.; Vartuli, J. C.; Roth, W. J.; Leonowicz, M. E.; Kresge, C. T.; Schmitt, K. D.; Chu, C. T.-W.; Olson, D. H.; Sheppard, E. W.; McCullen, S. B.; Higgins, J. B.; Schlenker, J. L. *J. Am. Chem. Soc.* **1992**, *114*, 10834. Kresge, C. T.; Leonowicz, M. E.; Roth, W. J.; Vartuli, J. C.; Beck, J. S. *Nature* **1992**, *359*, 710.

(2) Beck, J. S.; Vartuli, J. C.; Kennedy, G. J.; Kresge, C. T.; Roth, W. J.; Schramm, S. E. *Chem. Mater.* **1994**, *6*, 1816.

(3) Inagaki, S.; Fukushima, Y.; Kuroda, K. *J. Chem. Soc., Chem. Commun.* **1993**, 680.

(4) Monnier, A.; Schüth, F.; Huo, Q.; Kumar, D.; Margolese, D.; Maxwell, R. S.; Stucky, G. D.; Krishnamurty, M.; Petroff, P.; Firouzi, A.; Janicke, M.; Chmelka, B. F. *Science* **1993**, *261*, 1299.

(5) Chen, C.-Y.; Li, H.-X.; Davis, M. E. *Microporous Mater.* **1993**, *2*, 17.

(6) Chen, C.-Y.; Burkett, S. L.; Li, H.-X.; Davis, M. E. *Microporous Mater.* **1993**, *2*, 27. Davis, M. E.; Chen, C.-Y.; Burkett, S. L.; Lobo, R. F. In *Mater. Res. Soc. Symp. Proc.: Better Ceramics Through Chemistry VI*; Cheetham, A. K., et al., Eds.; MRS: Pittsburgh, 1994; p 831.

(7) Huo, Q.; Margolese, D. I.; Ciesla, U.; Feng, P.; Gier, T.; Sieger, P.; Leon, R.; Petroff, P. M.; Schüth, F.; Stucky, G. D. *Nature* **1994**, *368*, 317. Huo, Q.; Margolese, D. I.; Ciesla, U.; Demuth, D. G.; Feng, P.; Gier, T.; Sieger, P.; Firouzi, A.; Chmelka, B. F.; Schüth, F.; Stucky, G. D. *Chem. Mater.* **1994**, *6*, 1176.

S0897-4756(95)00549-7 CCC: $12.00 © 1996 American Chemical Society

assembly of cationic inorganic species ($I^+$) into $S^-I^+$ organic–inorganic biphase arrays. Two additional pathways involved counterion ($X^-$ or $M^+$)-mediated assemblies of surfactants and inorganic species of similar charge, namely, $S^+X^-I^+$ (where $X^- = Cl^-$ or $Br^-$) or $S^-M^+I^-$ (where $M^+ = Na^+$ or $K^+$) assembly, respectively. The viability of $S^+X^-I^+$ assembly was demonstrated by the synthesis of a hexagonal MCM-41 using a quaternary ammonium cationic template and strongly acidic conditions (5–10 M HCl or HBr) in order to generate and assemble positively charged framework precursors.[7]

We have proposed a neutral ($S^0I^0$) templating route[8] to mesoporous molecular sieves that is based on hydrogen bonding and self-assembly between neutral primary amine surfactants ($S^0$) and neutral inorganic precursors ($I^0$). This neutral $S^0I^0$ templating route afforded a distinguishable subset of hexagonal mesoporous molecular sieves (denoted HMS)[8] with physical and catalytic properties substantially different from MCM-41 materials prepared by electrostatic assembly. Although HMS materials clearly belong to the MCM-41 class of molecular sieves the difference in physical properties is sufficient, in our opinion, to justify the use of a different notation.

In the present work we report a detailed comparison of the physical properties of mesoporous MCM-41 silica molecular sieves obtained by electrostatic $S^+I^-$ and $S^+X^-I^+$ assembly processes with HMS silicas prepared by neutral $S^0I^0$ assembly. Besides differing fundamentally in framework charge, the two classes of materials exhibit important differences in short- and long-range order, framework cross-linking, framework wall thickness, thermal stability toward calcination in air, and $N_2$ sorption properties.

## Experimental Section

**Chemicals.** The sources of silica were N-brand sodium silicate solution, containing 29 wt % $SiO_2$, and tetraethyl orthosilicate (TEOS) obtained from P. Q. Corp. and Kodak, respectively. The surfactants were (i) quaternary ammonium salts with formula $C_nH_{2n+1}N(CH_3)_3Br$ (denoted as $C_n^+$) and (ii) primary amines with formula $C_nH_{2n+1}NH_2$ (denoted as $C_n^0$) where $n = 8$, 10, 12, 14, 16, and 18. The surfactants were obtained from Aldrich, Lancaster and TCI America. Sulfuric acid (96 wt %) was purchased from J. T. Baker Chemical Co. Hydrochloric acid (36–38 wt %) was obtained from EM Science. Absolute ethyl alcohol (EtOH) was used as a cosolvent during HMS synthesis and as a solvent during template removal by solvent extraction.

**Synthesis.** The following describes the specific synthesis procedures.

*MCM-41 by $S^+I^-$ Assembly.* These samples were prepared as described previously[2] using $C_nH_{2n+1}N(CH_3)_3Br$ surfactants with alkyl chain lengths $n = 8$, 10, 12, 14, and 16. Sodium silicate solution was used as a source of silica, and the pH of the reaction mixture was adjusted[2] with diluted sulfuric acid. In each case the reaction mixture had the following molar composition:

$$1.0\ SiO_2{:}0.5\ C_nH_{2n+1}N(CH_3)_3Br{:}0.31\ Na_2O{:}0.13H_2SO_4{:}n\ H_2O$$

The number of moles of water ($n$) in each reaction mixture were varied[2] in the range 54–64 mol for surfactants with alkyl chain length from $C_8^+$ to $C_{16}^+$, respectively. The synthesis of the samples was carried out by subjecting the reaction mixture to heating in an autoclave at 100 °C for 6 days or by aging it at ambient temperature for 7 days.

*MCM-41 by $S^+X^-I^+$ Assembly.*[7] For these modified preparations, the appropriate amount of $C_nH_{2n+1}N(CH_3)_3Br$ template ($n = 8$, 10, 12, 14, 16, 18) was dissolved in an acid/water mixture, followed by the addition of TEOS. The molar composition of a reaction mixture was

$$1.0\ TEOS{:}0.13\ C_nH_{2n+1}N(CH_3)_3Br{:}5.4\ HCl{:}150\ H_2O$$

The reaction mixture was aged under vigorous stirring at ambient temperature for 7 days in order to prepare the crystalline MCM-41 product.

*HMS by $S^0I^0$ Assembly.* These preparations were accomplished by hydrolysis of TEOS in the presence of $C_nH_{2n+1}NH_2$ primary amines ($n = 8$, 10, 12, 14, 16, 18), water, and EtOH as a cosolvent. The use of a cosolvent improved template solubility. In a typical preparation, TEOS was added to a vigorously stirred solution of amine in ethanol and deionized water, affording a reaction mixture of the following molar composition:

$$1.0\ TEOS{:}0.27\ C_nH_{2n+1}NH_2{:}9.09\ EtOH{:}29.6\ H_2O$$

The reaction mixture was aged at ambient temperature for 18 h in order to obtain the hexagonal mesoporous silica.

All ambient temperature syntheses were conducted by exposing the reaction mixture to the open atmosphere. Small amounts of deionized water were added during the aging process in order to compensate for the evaporation. The obtained crystalline products were recovered by filtration, washed with deionized water, and air-dried.

**Template Removal.** Template removal was achieved either by calcination in air at 630 °C for 4 h (heating rate 2 °C/min) or by solvent extraction. The solvent extraction was performed by stirring 1 g of the air-dried product in 150 mL of hot (45 °C) EtOH for 1 h. The product was then filtered and washed with another 100-mL portion of ethanol. This extraction procedure was repeated twice (the final extraction was performed in boiling EtOH), and the crystalline product was air-dried in an oven at 80 °C for 1 h. In some cases, complete cross-linking of the structure of the solvent-extracted materials was accomplished by subsequent calcination in air at 630 °C for 4 h (heating rate 2 °C/min).

**Analytical Techniques.** Powder X-ray diffraction patterns were measured on Rigaku Rotaflex diffractometer equipped with a rotating anode and using Cu Kα radiation.

Samples for TEM observation were prepared by embedding in L. R. White acrylic resin (hard) and sectioned on an ultramicrotome. The thin sections (~80 nm) were supported on 300 mesh copper grids and subsequently carbon coated to improve stability and reduce charging. The transmission electron micrographs were taken on a JEOL JEM-100CX II microscope equipped with lanthanum hexaboride ($LaB_6$) gun using an accelerating voltage of 120 kV and 20 $\mu$m objective lens aperture. The scanning electron micrographs were taken on a JEOL JSM 6400V using an accelerating voltage of 8 kV and a 16 mm working distance.

The $N_2$ adsorption–desorption isotherms were measured at −196 °C on a Coulter Omnisorp 360 CX Sorptometer using a continuous adsorption procedure. Before measurement, samples were evacuated overnight at 150 °C and $10^{-6}$ Torr. The BET surface area was calculated from the linear part of the BET plot according to IUPAC recommendations.[9] The pore size distribution was estimated from the adsorption branch of the isotherms by the method of Horvath and Kawazoe.[10]

$^{29}Si$ MAS NMR spectra were obtained on a Varian 400 VRX solid-state NMR spectrometer at 79.5 MHz using 7 mm zirconia rotors, a pulse delay of 800 s, and a sample spinning frequency of 4 kHz. The pulse delay time was determined by measuring the $T_1$ (relaxation time) value for each group of samples and selecting the larger measured value (120 s) as a base for the determination. Thus, all spectra were acquired with pulse delay of more than 6 times the maximum measured

---

(8) Tanev, P. T.; Pinnavaia, T. J. *Science* **1995**, *267*, 865.

(9) Sing, K. S. W.; Everett, D. H.; Haul, R. A. W.; Moscou, L.; Pierrotti, R. A.; Rouquérol, J.; Siemieniewska, T. *Pure Appl. Chem.* **1985**, *57*, 603.

(10) Horvath, G.; Kawazoe, K. J. *J. Chem. Eng. Jpn.* **1983**, *16*, 470.

$T_1$ value. The chemical shifts were referenced to TMS (tetramethylsilane). $^{14}N$ NMR spectra were recorded at 28.88 MHz on a Varian 400 VXR solid-state NMR spectrometer. Chemical shifts were referenced to an aqueous ammonium chloride solution. A quadrupole echo sequence with quadrature phase cycling was used with 90° pulse length of 4 $\mu$s and interpulse delay ($\tau$) of 115 to 120 $\mu$s. Depending on the sample, 30−20000 transients were collected with a spectral width of 200 kHz and a recycle time of 140 ms.

The TGA curves were recorded in air on a Cähn TG System 121 thermogravimeter using a heating rate of 5 °C/min.

## Results and Discussion

**Synthesis.** We have prepared two series of MCM-41 silicas by electrostatic $S^+I^-$ assembly processes using quaternary ammonium surfactants with different chain lengths. The first series of materials were prepared under hydrothermal conditions (100 °C) following the recipe given by Mobil,[2] whereas the second series was obtained by aging the reaction mixtures at ambient temperature.

We also have prepared a series of MCM-41 silicas by ambient temperature $S^+X^-I^+$ assembly[7] using different quaternary ammonium surfactants. Our attempts to prepare MCM-41 materials by $S^+X^-I^+$ assembly under reflux conditions, however, afforded instead very poorly ordered products and low product yields. Low yields (~25%) were characteristic of this pathway even at ambient temperature.

A series of HMS samples were prepared by ambient temperature $S^0I^0$ assembly using neutral primary amine surfactants with alkyl chain lengths equivalent to the cationic quaternary ammonium analogues. HMS silicas can be prepared in the temperature range from ambient up to 80 °C, but efforts to prepare these neutral framework materials under hydrothermal conditions at 100 °C afforded amorphous products. This is probably due to the weak H-bonding interactions between the surfactant head groups and the neutral inorganic precursor species and to the increased thermal disorder at elevated temperature.

In the discussions below we will compare the crystallinity of MCM-41 silicas prepared by $S^+I^-$ assembly at both ambient temperature and at 100 °C. All $S^+X^-I^+$ MCM-41 and the $S^0I^0$ HMS silicas, however, were prepared under ambient-temperature conditions where products with the best long-range order normally are formed.

**Crystallinity and Morphology.** Figure 1 shows the powder X-ray diffraction (XRD) patterns of the calcined HMS and MCM-41 silicas prepared using neutral and cationic surfactants of different alkyl chain length. Figure 1A indicates that all HMS materials prepared by $S^0I^0$ templating exhibit single $d_{100}$ reflections accompanied by more or less pronounced diffuse scattering centered at ~1.8 nm. Higher order Bragg reflections are not resolved in the patterns of the $S^0I^0$ HMS materials. However, we and others have demonstrated[8,11,12] that similar "single-reflection" materials can still exhibit local hexagonal symmetry as observed by selected area electron diffraction and TEM. We attribute the XRD behavior of HMS materials to small scattering domain sizes (see below) and to disorder resulting from the relatively weak, H bonding forces that operate in the $S^0I^0$ assembly process. As the surfactant chain length is increased from $C_8{}^0$ to $C_{18}{}^0$, the position of the [100] reflection shifts toward higher $d_{100}$ spacings. This result is not unexpected and implies that surfactants with longer alkyl chain lengths would afford materials with larger framework mesopore sizes.

The calcined forms of $S^+I^-$ MCM-41 silicas prepared at ambient temperature also exhibit relatively broad $d_{100}$ reflections and diffuse higher order scattering (see Figure 1B). This indicates a much lower degree of order in comparison to the $S^+I^-$ templated products prepared by hydrothermal treatment at 100 °C (see Figure 1C). These latter MCM-41 materials exhibit sharper $d_{100}$ reflections accompanied by diffuse scattering or, in some cases, additional 110, 200, and 210 reflections indicative of long-range ordered hexagonal framework.[1,2] It is noteworthy that for calcined forms of $S^+I^-$ MCM-41 silicas prepared at 100 °C, surfactant chain lengths of at least $C_{12}{}^+$ units are necessary in order to observe the well-resolved reflections indicative of hexagonal structure. On the other hand, the calcined (in air) form of the $S^+I^-$ MCM-41 prepared hydrothermally from a $C_{16}{}^+$ surfactant again shows broadened 110, 200, and 210 reflections, although these reflections are well resolved in the pattern for the corresponding as-synthesized material (not shown). This broadening of higher order reflections for $C_{16}{}^+$ templated $S^+I^-$ MCM-41 occurred even though the heating rate for calcination was low (2 °C/min). Perhaps the combustion of relatively large amounts of the organic surfactant phase during calcination in air (no pretreatment under $N_2$) of the $C_{16}{}^+$-templated MCM-41 leads to a local thermal destruction of the framework walls.

Figure 1D shows the powder XRD patterns of the calcined MCM-41 samples prepared at ambient temperature by the acidic $S^+X^-I^+$ pathway. All attempts to prepare MCM-41 materials by this pathway from $C_n{}^+$ surfactants with $n < 14$ afforded X-ray amorphous or very poorly ordered products. Surfactant chain lengths of at least $C_{16}{}^+$ units are necessary in order to observe the additional 110 and 200 reflections of the hexagonal phase. In contrast to the $S^+I^-$ pathway, $S^+X^-I^+$ assembly at ambient temperature affords very well ordered calcined MCM-41 products for surfactants of alkyl chain lengths $\geq C_{16}{}^+$. A comparison of XRD patterns for these calcined $S^+X^-I^+$ MCM-41 silicas with those for calcined $S^+I^-$ MCM-41 (Figure 1C) reveals another interesting fact. Different surfactant chain lengths are necessary in order to observe long-range hexagonal order in the two electrostatically templated reaction systems. This could be attributed to differences in (i) the pH conditions, (ii) the surfactant and inorganic reagents concentrations, (iii) the type of ions present in the reaction mixture, and (iv) the ionic strength of the solution. It may be that a combination of these parameters determines the surfactant chain conformations, the degree of hexagonal packing of micelles, the degree of framework cross-linking, and the crystallinity of the product.

The above XRD results clearly show that calcined forms of $S^+I^-$ MCM-41 silicas prepared by hydrothermal treatment at 100 °C exhibit better long-range hexagonal order than the corresponding products prepared by

---

(11) Tanev, P. T.; Chibwe, M.; Pinnavaia, T. J. *Nature* **1994**, *368*, 321.

(12) Beck, J. C.; Chu, C. T.-W.; Johnson, I. D.; Kresge, C. T.; Leonowicz, M. E.; Roth, W. J.; Vartuli, J. C. Int. Pat. Appl. WO 91/113090, 1991. Schmidt, R.; Akporiaye, D.; Stöcker, M.; Ellestad, O. H. In *Zeolites and Related Microporous Materials: State of the Art 1994*; Weitkamp, J., Karge, H. G., Pfeifer, H., Hölderich, W., Eds.; Elsevier Science: Amsterdam, 1994; p 61.

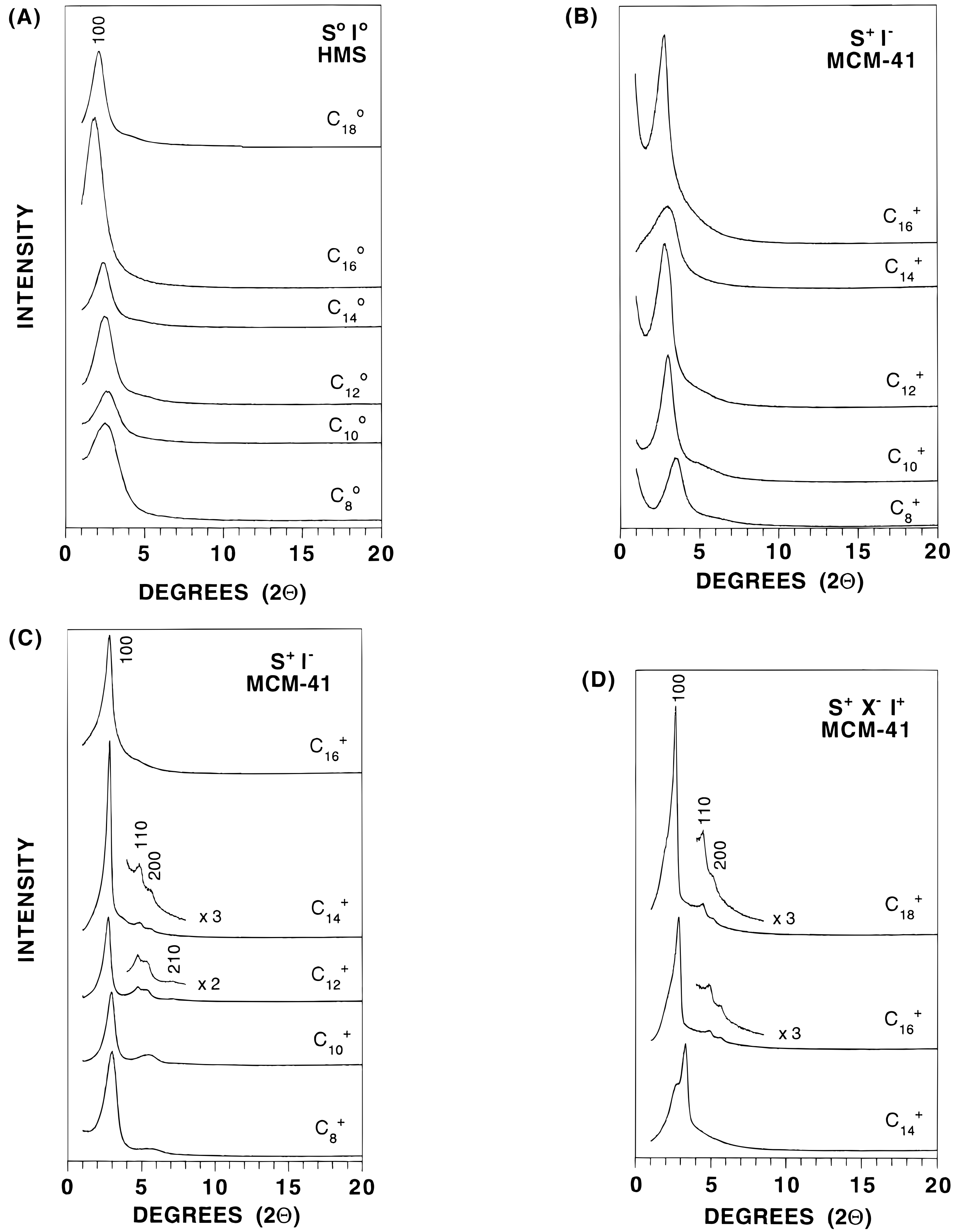

**Figure 1.** Powder XRD patterns of calcined mesoporous molecular sieves templated with neutral primary amine ($C_n^0$) and cationic alkyl trimethylammonium ($C_n^+$) surfactants of different alkyl chain lengths ($n = 8, 10, 12, 14, 16$, and 18). (A) HMS silicas prepared at ambient temperature by $S^0I^0$ assembly, (B) MCM-41 silicas prepared at ambient temperature by $S^+I^-$ assembly, (C) MCM-41 silicas prepared at 100 °C by $S^+I^-$ assembly, and (D) MCM-41 silicas prepared at ambient temperature by the counterion-mediated $S^+X^-I^+$ assembly.

ambient temperature synthesis. For these reasons our further comparisons of materials will consider only $S^+I^-$ MCM-41 silicas prepared by hydrothermal synthesis at 100 °C.

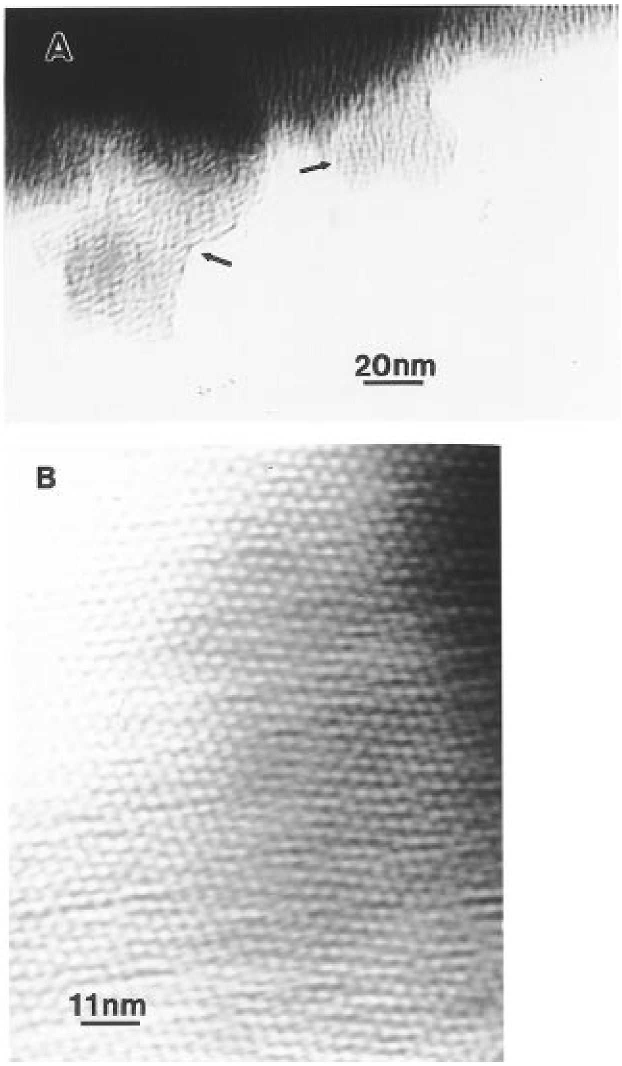

**Figure 2.** Representative TEM micrographs for calcined (A) $S^0I^0$ HMS prepared from $C_{12}{}^0$ as the surfactant and (B) $S^+X^-I^+$ MCM-41 prepared from $C_{16}{}^+$ as the surfactant.

Figure 2 shows representative TEM lattice images of HMS prepared by $S^0I^0$ templating and MCM-41 prepared by $S^+X^-I^+$ assembly. Both materials exhibit uniform framework-confined channels (mesopores), but MCM-41 shows long-range hexagonal ordering of the channels (image B), whereas in HMS the channels are arranged over a much shorter range in a hexagonal-like fashion (see arrows, image A). The size of the mesopores estimated by TEM is in agreement with the values determined from adsorption data (see below). Figure 3 shows representative SEM micrographs of calcined HMS (photo A) and MCM-41 samples (photos B and C). The materials exhibit very different morphologies. HMS consists of nonuniform aggregates of very small, distinct particles. In contrast, MCM-41 silicas prepared by $S^+I^-$ templating (at 100 °C) and by $S^+X^-I^+$ templating exhibit larger and much more monolithic aggregates (see photos B and C).

**Sorption Properties and Framework Wall Thickness.** Figure 4 shows the $N_2$ adsorption−desorption isotherms for calcined HMS and MCM-41 products prepared from surfactants of different alkyl chain lengths. For the purpose of simplifying the following discussion we define and differentiate the terms “framework-confined” mesoporosity and “textural” mesoporosity. The framework-confined mesoporosity is the porosity contained within the uniform channels of the templated framework. The size of framework-confined mesopores is equal to the diameter of the framework channels or to the diameter of the parent rodlike micelles and can be varied by changing the surfactant alkyl chain length or by the addition of auxiliary organics.[1−8] The presence of framework-confined mesopores is indicated by the adsorption step centered in the relative pressure ($P_i/P_0$) region from 0.1 to 0.5 in the $N_2$ isotherm (see, for example, Figure 4). A qualitative indication of the extent and the uniformity of the framework mesoporosity is provided by the height and steepness of the sorption step. Thus, the taller and sharper the adsorption step, the greater the amount of well-defined framework mesoporosity.

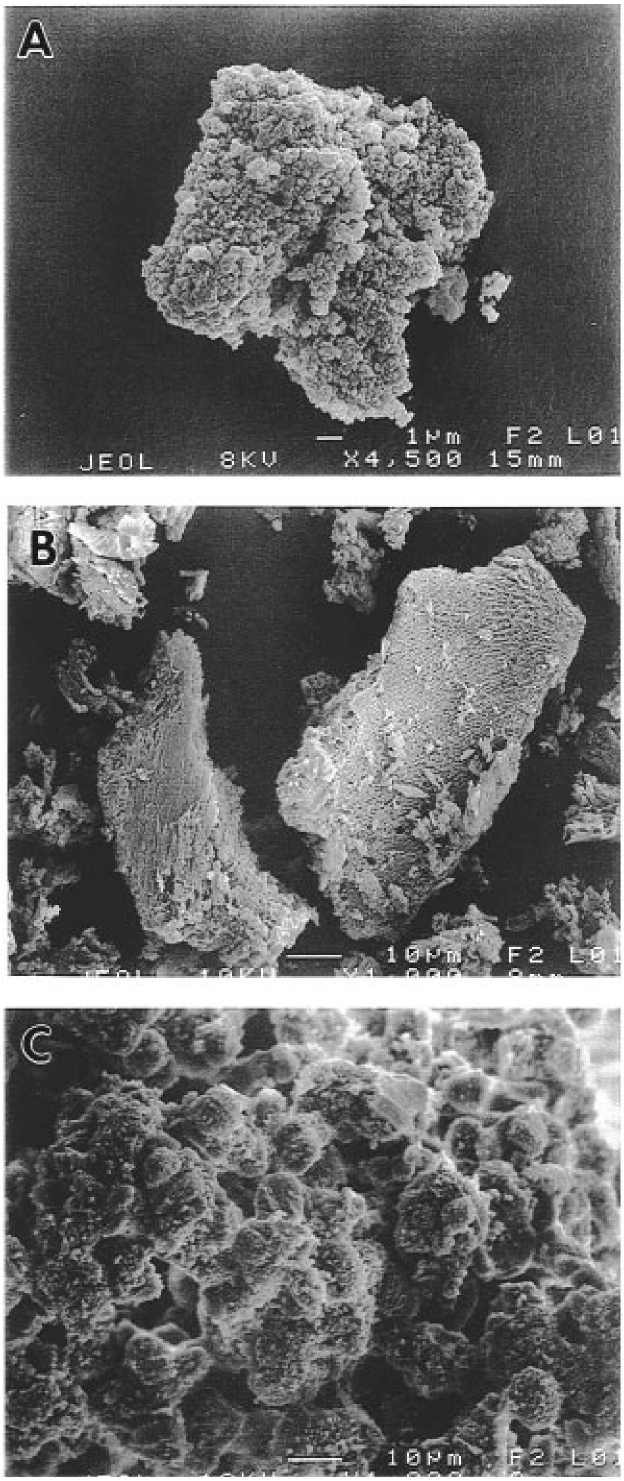

**Figure 3.** Representative SEM micrographs of calcined (A) $S^0I^0$ HMS, (B) $S^+I^-$ MCM-41 (prepared at 100 °C), and (C) $S^+X^-I^+$ MCM-41 samples.

**Table 1. Properties of Calcined Mesoporous Silicas Assembled by Different Templating Routes**[a]

| templating route | template alkyl chain length | $d_{100}$ (nm) | scattering domain size (nm) | $a_0$ (nm) | HK pore size (nm) | wall thickness (nm) |
|---|---|---|---|---|---|---|
| $S^0I^0$ | $C_8$ | 3.6 | 11.0 | 4.2 | 1.6 | 2.6 |
| $S^0I^0$ | $C_{10}$ | 3.4 | 15.7 | 3.9 | 2.0 | 1.9 |
| $S^0I^0$ | $C_{12}$ | 3.6 | 17.0 | 4.2 | 2.4 | 1.8 |
| $S^0I^0$ | $C_{14}$ | 3.7 | 15.4 | 4.3 | 2.2 | 2.1 |
| $S^0I^0$ | $C_{16}$ | 4.8 | 11.4 | 5.5 | 2.5 | 3.0 |
| $S^0I^0$ | $C_{18}$ | 4.2 | 14.5 | 4.8 | 3.1 | 1.7 |
| $S^+I^-$ | $C_8$ | 2.8 | | 3.2 | 1.7 | 1.5 |
| $S^+I^-$ | $C_{10}$ | 3.0 | 34.0 | 3.5 | 2.1 | 1.4 |
| $S^+I^-$ | $C_{12}$ | 3.2 | 52.0 | 3.7 | 2.4 | 1.3 |
| $S^+I^-$ | $C_{14}$ | 3.1 | 102.6 | 3.6 | 2.1 | 1.5 |
| $S^+I^-$ | $C_{16}$ | 3.1 | 90.0 | 3.6 | 2.2 | 1.4 |
| $S^+I^-$ | $C_{18}$ | amorph | | | | |
| $S^+X^-I^+$ | $C_{14}$ | 2.7 | | 3.1 | | |
| $S^+X^-I^+$ | $C_{16}$ | 3.1 | 53.0 | 3.6 | 2.2 | 1.4 |
| $S^+X^-I^+$ | $C_{18}$ | 3.4 | 66.2 | 3.9 | 2.7 | 1.2 |

[a] The scattering domain size was determined from the line width of the $d_{100}$ X-ray reflection. The repeat distance ($a_0$) between pore centers of the hexagonal structure is calculated from the XRD data using the formula $a_0 = 2d_{100}/\sqrt{3}$. The framework-confined mesopore size (HK pore size) was determined by Horvath–Kawazoe (HK) analysis of the $N_2$ adsorption isotherms.[10] The framework wall thickness is determined by subtracting the HK mesopore size from the repeat distance between pore centers.

Textural mesoporosity is the porosity arising from non crystalline intraaggregate voids and spaces formed by interparticle contacts. Each of the fundamental particles in the case of HMS and MCM-41 molecular sieves is composed of a certain number of framework unit cells or framework-confined mesopores. The size of the textural mesopores is determined in large part by the size, shape, and number of interfacial contacts within the aggregates. Usually, the size of the textural mesopores are at least 1 order of magnitude larger than the framework-confined mesopores. The presence of textural mesoporosity is verified by the appearance of a well-defined hysteresis loop in the $N_2$ adsorption–desorption isotherms in the $P_i/P_0$ region from 0.5 to 1.0.

The $N_2$ adsorption–desorption isotherms for HMS silicas are shown in Figure 4A. All materials, regardless of the surfactant alkyl chain length, exhibit substantial framework-confined and textural mesoporosity. However, the shorter alkyl chain lengths ($C_8^0$–$C_{10}^0$) afford more textural mesoporosity relative to framework-confined mesoporosity, whereas the reverse is true for longer alkyl chain surfactants. Surfactants with intermediate chain length (such as $C_{12}^0$) seem to give textural mesoporosity comparable in volume to the framework-confined mesoporosity.

The $N_2$ adsorption–desorption isotherms for $S^+I^-$ MCM-41 silicas are shown in Figure 4B. Again, shorter alkyl chain lengths generally afford a higher fraction of textural mesoporosity, whereas longer alkyl chains generally tend to limit textural mesoporosity. However, the fraction of textural mesoporosity exhibited by these electrostatically templated samples is very small relative to HMS materials prepared from neutral amine surfactants with equivalent chain lengths. MCM-41 silicas prepared by the acidic $S^+X^-I^+$ assembly exhibit $N_2$ sorption isotherms similar to those of the $S^+I^-$ electrostatic counterparts. These products also lack appreciable textural mesoporosity (see Figure 4C).

On the basis of the above XRD and $N_2$ adsorption data, we are now able to summarize some of the key structural properties of calcined HMS and MCM-41 silica molecular sieves. The data in Table 1 indicate the following general trends: (i) all $S^0I^0$ HMS materials templated by neutral primary amines with alkyl chain lengths from $C_8^0$ to $C_{18}^0$ exhibit $d_{100}$ and hexagonal lattice parameters ($a_0$) values that are larger than those for the corresponding MCM-41 samples prepared from ionic surfactants of the same alkyl chain length; (ii) the scattering domain sizes of the neutral HMS derivatives are smaller ($\leq$17 nm) than those of the corresponding ionic MCM-41 materials ($\geq$34 nm); (iii) the HK framework-confined mesopore sizes are similar for both classes of materials prepared with surfactants of equivalent alkyl chain length; (iv) the framework wall thicknesses of HMS mesostructures ($\geq$1.7 nm) are consistently larger than those of MCM-41 materials prepared from charged templates of equivalent alkyl-chain length.

The thin framework walls of $S^+I^-$ MCM-41 materials have been attributed[7] to the *limiting effects* of both the electrostatic repulsions between anionic silicate oligomers at the surfactant surface, and the $S^+I^-$ surfactant–silicate charge-matching interactions needed to maintain electrical neutrality during the mesostructure assembly process. Thus, the $S^+I^-$ MCM-41 wall growth process is terminated when charge compensation is achieved. The framework wall thickness of $S^+X^-I^+$ MCM-41 silicas is also limited by similar electrostatic interactions. Generally, both $S^+I^-$ and $S^+X^-I^+$ MCM-41 materials exhibit framework wall thicknesses in the range 1.2–1.5 nm (see Table 1). This observation is in agreement with the findings of Stucky et al. (0.8 to 0.9 nm)[7] and Davis and co-workers (~1.0 nm).[5,6] It has been emphasized[13] that MCM-41 materials with larger framework wall thicknesses are desirable because of improved thermal stability. Thus, the thin framework walls of electrostatically templated MCM-41 materials could limit their thermal and hydrothermal stability in adsorption and catalytic applications requiring severe regeneration conditions. The much thicker framework walls of the HMS materials prepared by the $S^0I^0$ pathway may be expected to afford superior thermal and hydrothermal stability relative to MCM-41 materials prepared by electrostatic templating.

Table 2 summarizes the quantitative sorption properties of HMS and MCM-41 mesoporous silicas. Both classes of materials exhibit similar BET specific surface areas ($S_{BET}$) and framework-confined mesopore volumes ($V_{fr}$). However, as we have seen earlier from a qualitative comparison of the $N_2$ adsorption isotherms, the materials differ quite significantly in total pore volume ($V_t$), textural mesopore volume ($V_{tex}$), and the ratio of textural to framework-confined mesoporosity ($V_{tex}/V_{fr}$). Thus, the HMS silicas exhibit much larger values of $V_t$, $V_{tex}$, and $V_{tex}/V_{fr}$ relative to the electrostatically templated MCM-41 samples. In addition, neutral templating allows for a large variation in the ratio of $V_{tex}/V_{fr}$ mesoporosity, whereas electrostatic templating affords uniformly low values for this ratio.

We emphasize that the enhanced textural mesoporosity in the case of HMS is a consequence of the small crystallite size and disorder in channel packing. The comparison of the data in Table 2 shows that the textural mesoporosity ($V_{tex}$) of HMS materials is truly complementary and does not occur at the expense of framework-confined mesoporosity ($V_{fr}$). This is evi-

---

(13) Coustel, N.; di Renzo, F.; Fajula, F. *J. Chem. Soc., Chem. Commun.* **1994**, 967.

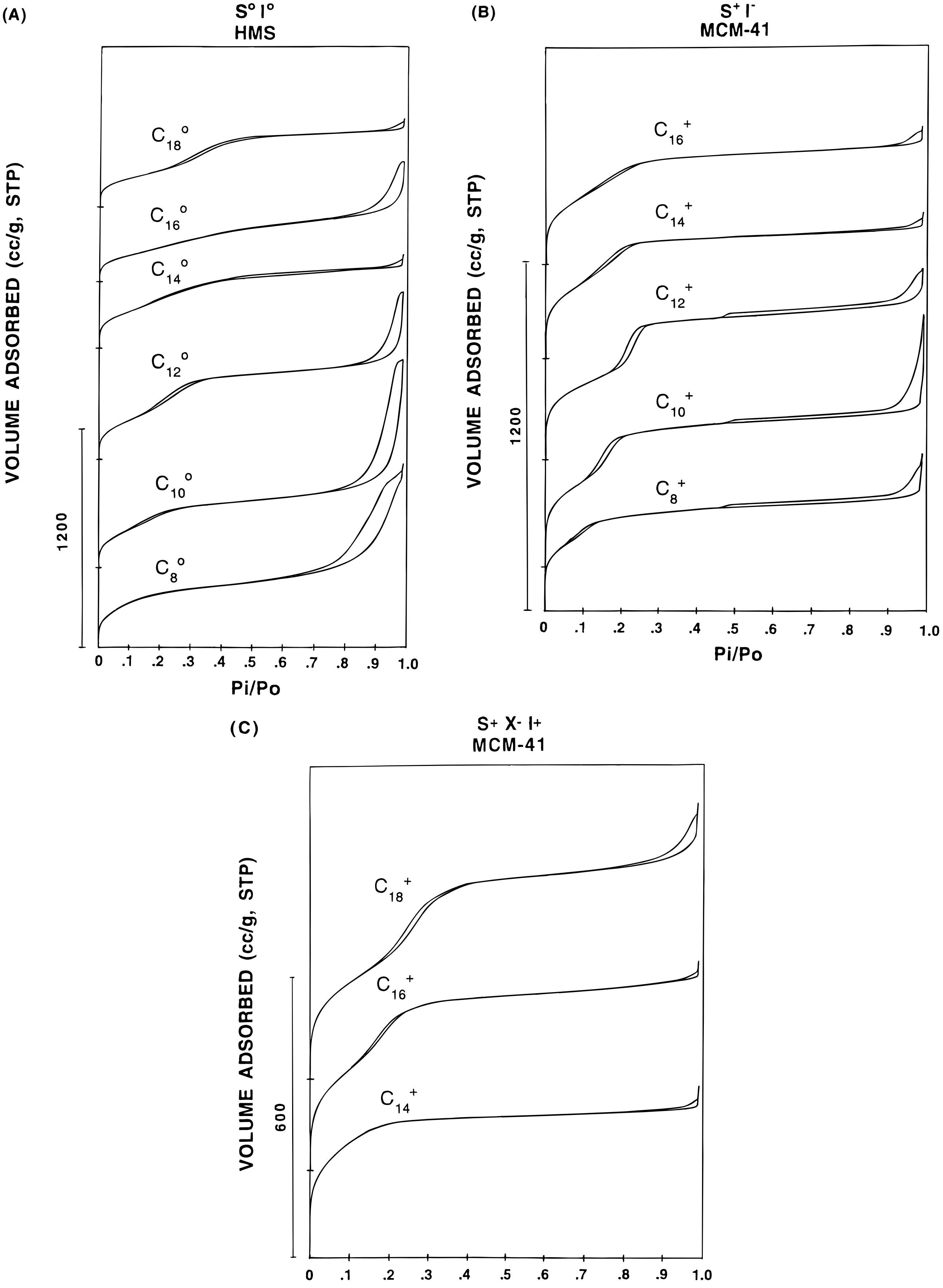

**Figure 4.** $N_2$ adsorption−desorption isotherms for calcined (A) $S^0I^0$ HMS silicas prepared with neutral ($C_n^0$) primary amine surfactants with $n = 8, 10, 12, 14, 16, 18$; (B) calcined $S^+I^-$ MCM-41 silicas prepared at 100 °C with cationic quaternary ammonium ($C_n^+$) surfactants with $n = 8, 10, 12, 14, 16$; and (C) $S^+X^-I^+$ MCM-41 silicas prepared with cationic quaternary ammonium ($C_n^+$) surfactants with $n = 14, 16, 18$.

**Table 2. Sorption Properties of Calcined Mesoporous Silicas Assembled by Different Templating Routes**

| templating route | template alkyl chain length | $S_{BET}$ (m$^2$/g) | $V_t$ (cm$^3$/g) | $V_{fr}$ (cm$^3$/g) | $V_{tex}$ (cm$^3$/g) | $V_{tex}/V_{fr}$ |
|---|---|---|---|---|---|---|
| $S^0I^0$ | $C_8$ | 1043 | 1.45 | 0.47 | 0.98 | 2.10 |
| $S^0I^0$ | $C_{10}$ | 1202 | 1.75 | 0.53 | 1.22 | 2.31 |
| $S^0I^0$ | $C_{12}$ | 1150 | 1.40 | 0.70 | 0.70 | 1.00 |
| $S^0I^0$ | $C_{14}$ | 1066 | 0.75 | 0.50 | 0.25 | 0.50 |
| $S^0I^0$ | $C_{16}$ | 740 | 1.01 | 0.40 | 0.60 | 1.50 |
| $S^0I^0$ | $C_{18}$ | 763 | 0.73 | 0.62 | 0.11 | 0.18 |
| $S^+I^-$ | $C_8$ | 1109 | 0.59 | 0.45 | 0.14 | 0.31 |
| $S^+I^-$ | $C_{10}$ | 1250 | 0.96 | 0.69 | 0.27 | 0.39 |
| $S^+I^-$ | $C_{12}$ | 1154 | 0.89 | 0.70 | 0.19 | 0.27 |
| $S^+I^-$ | $C_{14}$ | 1218 | 0.69 | 0.59 | 0.10 | 0.17 |
| $S^+I^-$ | $C_{16}$ | 1147 | 0.65 | 0.53 | 0.12 | 0.23 |
| $S^+I^-$ | $C_{18}$ | amorph | | | | |
| $S^+X^-I^+$ | $C_{14}$ | 1014 | 0.48 | 0.42 | 0.06 | 0.14 |
| $S^+X^-I^+$ | $C_{16}$ | 1104 | 0.70 | 0.59 | 0.11 | 0.19 |
| $S^+X^-I^+$ | $C_{18}$ | 1048 | 0.90 | 0.72 | 0.18 | 0.25 |

denced by the very similar values of $V_{fr}$ exhibited by the HMS and MCM-41 materials prepared with surfactants of equivalent alkyl chain length. In contrast, poorly ordered MCM-41 reaction products formed in the presence of a $C_{16}{}^+$ surfactant exhibit little or no framework-confined mesoporosity.[14,15] The lack of textural mesoporosity for MCM-41 silicas prepared by electrostatic templating pathways could limit access to the framework-confined mesopores and impose diffusional limitations on the adsorption and catalytic properties of these materials, especially in liquid-phase processes involving bulky organic molecules.[11]

**$^{29}$Si MAS NMR.** Recently, Mobil scientists reported the $^{29}$Si MAS NMR of as-synthesized M41S silicas prepared by the electrostatic $S^+I^-$ pathway.[16] Using deconvolution techniques, they resolved three broad, overlapping peaks in the spectra of hexagonal MCM-41 and cubic MCM-48 and two peaks in the spectra of thermally unstable lamellar MCM-50. The spectra for both MCM-41 and MCM-48 were essentially the same as for silica gel. This is not surprising given the amorphous character of the framework walls and the expected wide range of Si−O−Si bond angles. Interestingly, all as-synthesized $S^+I^-$ phases exhibited more noncondensed $Q^2$ and $Q^3$ $Si(SiO)_x(OH)_{4-x}$ framework units (where $x = 2$ or 3, respectively) than fully condensed $Q^4$ ($x = 4$) units. The $Q^4/Q^2 + Q^3$ values were typically near 0.67.[16] This result is extremely significant and implies a relatively *low degree of cross-linking* for the *as-synthesized* negatively charged $S^+I^-$ MCM-41 framework. A low degree of framework cross-linking is also evident from the results of Davis et al.[5,6] for as-synthesized MCM-41 ($Q^4/Q^2 + Q^3 \sim 0.77$). These latter workers first suggested that 100% $Q^4$ cross-linking of the $S^+I^-$ MCM-41 framework cannot be reached because the unlinked $SiO^-$ groups *are needed* for charge compensation of the cationic quaternary ammonium template ($S^+$).

The previously reported $^{29}$Si MAS NMR spectra of as-synthesized MCM-41 phases prepared by the counterion-mediated $S^+X^-I^+$ assembly exhibited slightly larger $Q^4/Q^3$ connectivity ratios (0.88−1.7).[7] Here the positive charge on the surfactant is partially balanced by an excess of halide counterions. This ion pairing allows for displacement of ~85 wt % of the template−halide ion pairs by solvent extraction.[7]

Figure 5 shows the $^{29}$Si MAS NMR spectra of our as-synthesized, ethanol-extracted, and calcined mesoporous molecular sieves prepared by neutral and electrostatic templating. The spectrum of the as-synthesized HMS material (A) reveals a much larger $Q^4/Q^3$ ratio (2.68) or much more highly cross-linked framework than the electrostatic MCM-41 counterparts (spectra B and C). The low $Q^4/Q^3$ ratios of 0.71 and 1.18 exhibited by as-synthesized $S^+I^-$ and $S^+X^-I^+$ MCM-41 silicas, respectively, are in good agreement with previously reported studies (see above). The comparison of the $^{29}$Si MAS NMR spectra of the ethanol-extracted samples further emphasizes the differences between neutral and charged framework structures. Thus, ethanol extraction seems to enhance the cross-linking of the HMS sample ($Q^4/Q^3 = 3.08$), whereas such treatment leads to a deterioration of the cross-linking for the electrostatically templated MCM-41 samples ($Q^4/Q^3 = 0.60$ and 1.04, respectively).

The comparison of the $^{29}$ Si MAS NMR spectra of the as-synthesized and calcined samples emphasizes yet another important point. The ratio of $Q^4/Q^3$ for $S^0I^0$ material does not change significantly upon calcination (compare spectral series A in Figure 5). This observation is not surprising in view of the lack of electrostatic repulsions and charge matching and the corresponding thicker pore walls of HMS materials prepared by neutral templating. The fact that the amount of noncondensed $Q^3$ units remains essentially unchanged upon calcination may indicate that a substantial fraction of $(SiO)_3\mathit{Si}{-}OH$ groups are incorporated in the thicker pore walls, as opposed to being located exclusively at the channel surfaces.

It recently has been reported that the pH adjustment of a $S^+I^-$ reaction mixture[17] with acetic acid (pH ~ 11) or a postsynthesis treatment of the $S^+I^-$ reaction product with HCl vapor[18] leads to significant enhancement in the cross-linking of MCM-41 silicas. Although these approaches may provide for the preparation of more cross-linked and potentially more stable $S^+I^-$ MCM-41 silicas, they share some of the disadvantages of the acidic $S^+X^-I^+$ assembly approach by requiring special reactor equipment and waste-disposal considerations in potential large-scale preparations.

**Template Removal and Thermal Stability toward Calcination in Air.** Figure 6 shows the powder XRD patterns of as-synthesized, ethanol-extracted, and ethanol-extracted and calcined mesoporous silica molecular sieves prepared by neutral and electrostatic templating pathways. The XRD data for HMS materials (see Figure 6A) clearly indicate preservation of the structure upon template removal by solvent extraction. It is remarkable that subsequent calcination of the ethanol-extracted sample did not affect the crystallinity of the product. We note that the intensities of the $d_{100}$ reflections of the ethanol-extracted and the ethanol-extracted and calcined HMS products are 4 times those for as-synthesized HMS. This is probably due to the more completely cross-linked framework of the HMS materials and to efficient removal of the neutral tem-

---

(14) Chen, C.-Y.; Xiao, S.-Q.; Davis, M. E. *Microporous Mater.* **1995**, *4*, 1.

(15) Lin, W.; Chen, J.; Sun, Y.; Pang, W. *J. Chem. Soc., Chem. Commun.* **1995**, 2367.

(16) Vartuli, J. C.; Schmitt, K. D.; Kresge, C. T.; Roth, W. J.; Leonowicz, M. E.; McCullen, S. B.; Hellring, S. D.; Beck, J. S.; Schlenker, J. L.; Olson, D. H.; Sheppard, E. W. *Chem. Mater.* **1994**, *6*, 2317.

(17) Ryoo, R.; Kim, J. M. *J. Chem. Soc., Chem. Commun.* **1995**, 711.

(18) Fyfe, C. A.; Fu, G. *J. Am. Chem. Soc.* **1995**, *117*, 9709.

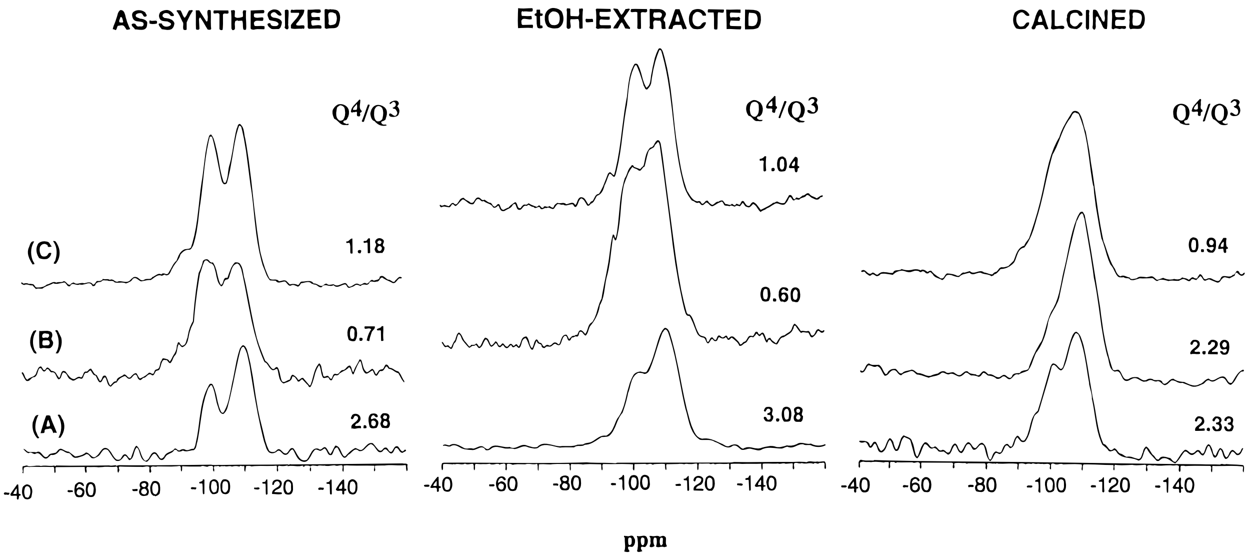

**Figure 5.** $^{29}$Si MAS NMR spectra of as-synthesized, ethanol-extracted and calcined samples of (A) $S^0I^0$ HMS, (B) $S^+I^-$ MCM-41 (prepared at 100 °C), (C) $S^+X^-I^+$ MCM-41.

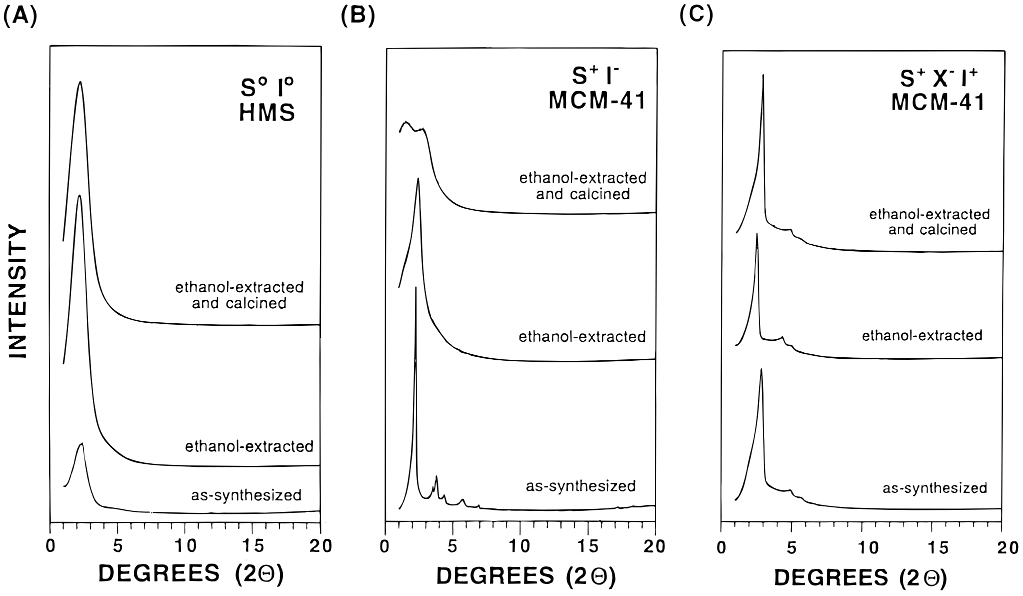

**Figure 6.** Powder XRD patterns of as-synthesized, ethanol-extracted, and ethanol-extracted and calcined mesoporous molecular sieves. (A) $S^0I^0$ HMS, (B) $S^+I^-$ MCM-41 (prepared at 100 °C), and (C) $S^+X^-I^+$ MCM-41. HMS was prepared from $C_{12}{}^0$ as the surfactant and $C_{16}{}^+$ was the surfactant for the electrostatically templated MCM-41 samples.

plate, which precludes the possibility of local heating and partial structural collapse upon calcination. This suggests that the preferred method for template removal from neutral HMS materials should be ethanol extraction followed by calcination.

Our attempts to remove the cationic template from $S^+I^-$ MCM-41 by ethanol extraction resulted in a significant broadening of the corresponding XRD reflections (see Figure 6B). It is noteworthy that subsequent calcination resulted in almost complete decomposition of the structure. These observations are in accord with the low degree of framework cross-linking in these electrostatically assembled mesostructures. As illustrated by Figure 6C, the crystallinity of the MCM-41 sample prepared by the acidic $S^+X^-I^+$ pathway is unaltered after template removal by ethanol extraction and subsequent calcination. This is probably caused by the successful displacement of most of the template–halide ion pairs ($S^+$ $X^-$) by solvent extraction.

Figure 7 shows the TGA curves of as-synthesized, ethanol-extracted, and ethanol-extracted and calcined mesoporous silicas prepared by neutral and electrostatic templating pathways. The curves for $S^0I^0$ HMS samples are depicted in Figure 7A. Several weight loss features can be distinguished. The region from ~20 to 150 °C is attributable to desorption of water, the second region from ~150 to 300 °C to the decomposition and combustion of the organic template, and the third from ~300 to 520 °C to dehydroxylation of the surface. However, the expanded TGA curve of the ethanol-extracted HMS (shown in Figure 7A as insert), clearly lacks inflection points indicative of template weight loss. This result suggests that the neutral template can be removed almost completely and recycled from the framework of the HMS materials by simple solvent extraction.

In contrast to the ethanol-extracted HMS, the TGA curve for the ethanol-extracted MCM-41 sample prepared by $S^+I^-$ templating (see Figure 7B) indicates more than a 25% weight loss due to decomposition and combustion of remaining cationic template. This implies that the framework of the as-synthesized $S^+I^-$ MCM-41 materials is negatively charged and that the

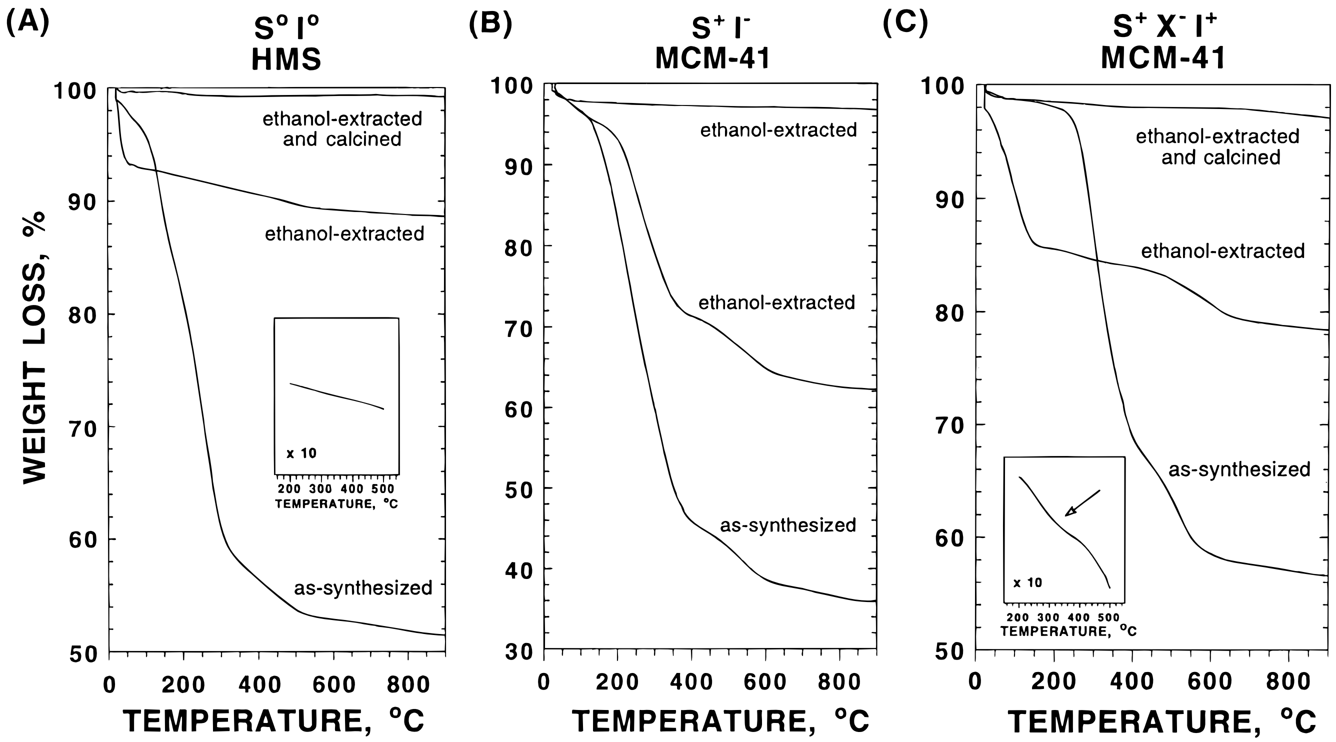

**Figure 7.** TGA curves of as-synthesized, ethanol-extracted, and ethanol-extracted and calcined mesoporous molecular sieves. (A) $S^0I^0$ HMS, (B) $S^+I^-$ MCM-41 (prepared at 100 °C), and (C) $S^+X^-I^+$ MCM-41. HMS was prepared from $C_{12}^0$ as the surfactant and $C_{16}^+$ was the surfactant for the electrostatically templated MCM-41 samples.

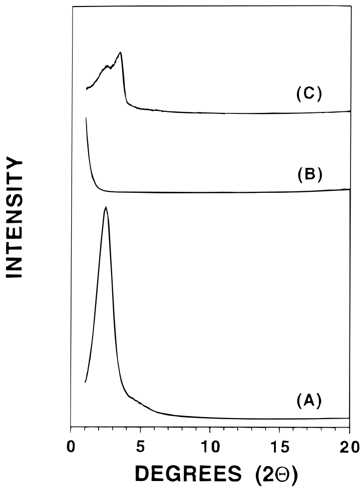

**Figure 8.** Powder XRD patterns of (A) $S^0I^0$ HMS, (B) $S^+I^-$ MCM-41 (prepared at 100 °C), and (C) $S^+X^-I^+$ MCM-41 samples calcined in air at 900 °C for 4 h. HMS was prepared from $C_{12}^0$ as the surfactant and $C_{16}^+$ was the surfactant for the electrostatically templated MCM-41 samples.

cationic template is strongly bound to the framework and difficult to recover.

In accord with the findings of Stucky and co-workers,[7] we also find that most of the template–halide ion pairs of the acidic $S^+X^-I^+$ MCM-41 materials are displaced by simple solvent extraction. This is evident from the TGA curves presented in Figure 7C. However, the expanded TGA curve for the ethanol-extracted MCM-41 (see insert) shows inflection points due to template weight loss. This probably indicates that small amount of the cationic template remains strongly and directly bound to the framework of the $S^+X^-I^+$ molecular sieves.

To compare the thermal stability of the mesoporous molecular sieves prepared by neutral and electrostatic templating pathways, we have subjected representative samples to calcination in air at 900 °C for 4 h. The XRD patterns of the calcined samples are presented in Figure 8. The framework of the electrostatic $S^+I^-$ MCM-41 sample completely collapses upon this thermal treatment. Significant structural collapse was also reported for the $H^+$-exchanged $S^+I^-$ MCM-41 samples at temperatures above 850 °C.[5] The structure of the $S^+X^-I^+$ MCM-41 analog also is severely altered. In contrast, the thicker-walled and more completely cross-linked HMS sample prepared by neutral $S^0I^0$ templating retains its crystallinity after calcination in air at 900 °C for 4 h. This indicates that neutral templating may provide for the preparation of mesoporous molecular sieves with enhanced thermal stability to calcination in air.

**Mechanistic Considerations.** We have postulated[8] that the formation of neutral HMS mesostructures occurs through the organization of neutral primary amine surfactant molecules ($S^0$) and neutral $Si(OC_2H_5)_{4-x}(OH)_x$ precursors into rodlike assemblies as depicted in Figure 9. H-bonding interactions between the precursor silanol hydrogens and the lone electron pairs on the surfactant head groups changes the head-to-chain volume ratio (i.e., the preferred packing) of the surfactant–inorganic complexes and most likely facilitates the assembly of rodlike micelles. Further hydrolysis and condensation of the silanol groups on the micelle–solution interface afford short-range hexagonal packing of the micelles and framework wall formation. We cannot preclude the possibility of a slightly different pathway involving preorganized spherical micelles or even surfactant bilayer arrays in our ethanol–water solutions of template. Even in these latter cases, however, we expect a rodlike assembly process to be initiated by H-bonding interactions between the surfactant and the intermediate silica precursor species.

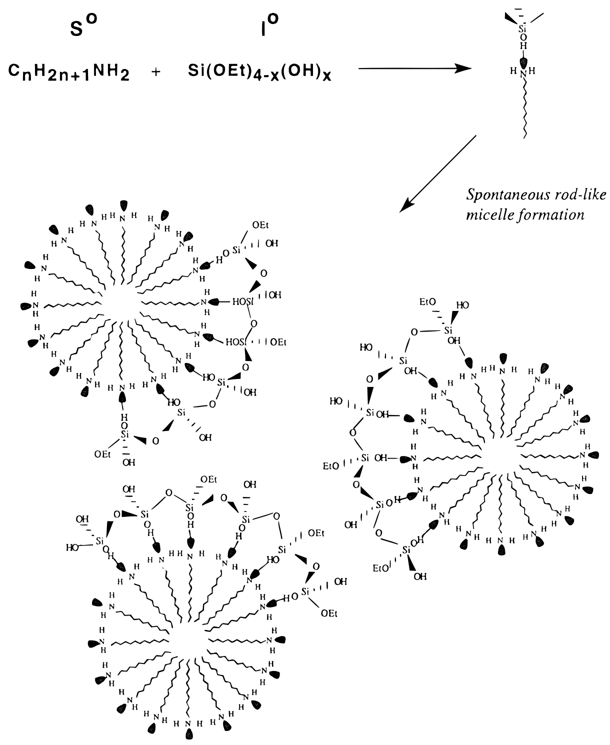

**Figure 9.** Schematic representation of the $S^0I^0$ templating mechanism of formation of HMS mesoporous molecular sieves. The shaded lobes on the surfactant head groups are electron lone pairs that participate in H bonding with framework silanols.

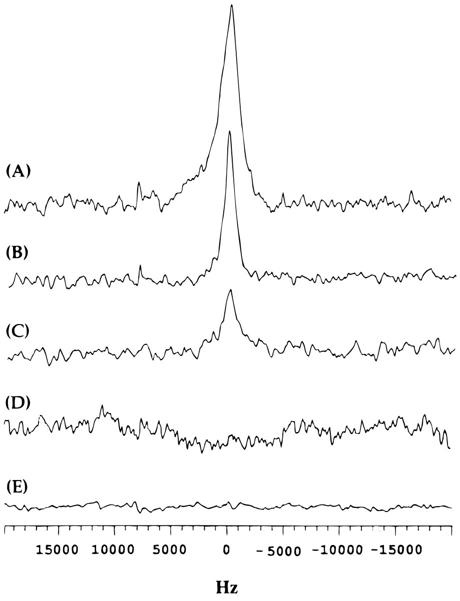

**Figure 10.** $^{14}$N NMR spectra of (A) aqueous solution of intentionally protonated DDA (molar composition 0.27 DDA: 0.054 HCl:9.09 EtOH:29.6 $H_2O$), (B) the supernatant liquid separated from the $HMS^+$ reaction product prepared from templating solution (A), (C) the wet $HMS^+$ solid product separated from the reaction product obtained from templating solution (A), (D) our neutral templating solution (molar composition 0.27 DDA:9.09 EtOH:29.6 $H_2O$), and (E) fresh HMS reaction product prepared from templating solution (D).

Additional evidence in support of the postulated $S^0I^0$ mechanism was obtained by $^{14}$N NMR spectroscopy of neutral and intentionally protonated dodecylamine (DDA) solutions and corresponding HMS reaction products. Figure 10 shows the $^{14}$N NMR spectra of the above samples. By analogy to the reported spectra of aqueous cetyltrimethylammonium cation solutions,[6] the $^{14}$N NMR spectrum of the intentionally protonated DDA solution (spectrum A; 0.27 DDA:0.054 HCl:9.09 EtOH: 29.6 $H_2O$) exhibits a single isotropic resonance due to the $^{14}$N nucleus in a tetrahedral environment (one-fifth of the DDA intentionally protonated). We have used this partially protonated DDA solution to prepare a $HMS^+$ templated product. Further we separated the wet $HMS^+$ product from the supernatant liquor by centrifugation. The spectra of both the separated supernatant liquor (B) and wet $HMS^+$ reaction product (C) exhibit the single isotropic resonance clearly indicating the presence of protonated amine. This suggests that significant concentrations of protonated amine should readily be detected by the applied $^{14}$N NMR technique. In the absence of tetrahedral symmetry the signal produced by the $^{14}$N nucleus is broad and cannot be detected.[6] Because the $^{14}$N NMR spectrum of our neutral DDA templating solution and corresponding HMS product are featureless (see spectra D and E, respectively), the fraction of nitrogen centers adopting tetrahedral environment is negligible. This result further verifies that the mechanism of formation of the HMS mesoporous molecular sieves is predominantly neutral.

## Conclusions

$S^+I^-$ templating of anionic MCM-41 silicate frameworks occurs with greater long-range hexagonal order when the assembly process is carried out under hydrothermal reaction conditions (100 °C) rather than at ambient temperatures. On the other hand, MCM-41 silicas with well expressed hexagonal order are formed by $S^+X^-I^+$ assembly under ambient reaction conditions; hydrothermal $S^+X^-I^+$ assembly at 100 °C affords very poorly ordered products and low product yields. Neutral HMS silica molecular sieves are best prepared by $S^0I^0$ templating at ambient temperature; hydrothermal reactions at 100 °C afford only amorphous products. The lack of mesostructure formation at high reaction temperature in the case the $S^+X^-I^+$ ion pairing and $S^0I^0$ H-bonding pathways is attributable to relatively weak assembly forces that are obscured by thermal motions at elevated temperatures. In contrast, $S^+I^-$ ion pairing is sufficiently persistent under hydrothermal conditions to allow for long-range hexagonal assembly.

Owing to the strong electrostatic interactions between the anionic framework and the cationic surfactant in as-synthesized $S^+I^-$ MCM-41 derivatives, the surfactant can be removed only by proton ion exchange or calcination. Most of the framework template in $S^+X^-I^+$ MCM-41 derivatives is removable as template−halide ion pairs by solvent extraction, but the removal of the small portion of remaining electrostatically bound template requires ion exchange or calcination. In accord with the electrically neutral framework of $S^0I^0$ HMS silicas, the template can be subjected to effective and environmentally benign recovery and direct recycling by solvent extraction. $^{14}$N NMR spectroscopic studies of neutral and intentionally protonated primary amine HMS reaction mixtures provide additional support for the predominantly neutral character of the $S^0I^0$ assembly mechanism. Template removal by solvent extraction is a significant structural advantage, because it avoids the local damage that can be caused in removing the template by calcination.

All of the $S^0I^0$ HMS materials templated by neutral primary amines with alkyl chain lengths from $C_8{}^0$ to

$C_{18}{}^0$ exhibit $d_{100}$ and corresponding hexagonal lattice parameters ($a_0$) values that are larger than those for the corresponding MCM-41 samples prepared from ionic surfactants of the same alkyl chain length. The framework-confined mesopore sizes are similar for both classes of materials. Consequently, the framework wall thicknesses of HMS mesostructures (1.7−3.0 nm) are consistently larger than those of MCM-41 materials (1.2−1.5 nm) prepared from surfactants of the same chain length. Electrostatically templated MCM-41 silicas exhibit greater long-range hexagonal order than neutral HMS analogues, but both classes of materials show *uniform* framework mesopore distributions. That is, the uniformity of the framework pore structure is not substantially influenced by the fidelity of the long-range hexagonal order. Also, relative to electrostatically templated as-synthesized MCM-41 derivatives, HMS silicas exhibit more extensively cross-linked frameworks, which, together with the thicker framework walls, contributes to superior thermal stability in calcination in air. In addition, the scattering domain sizes of the neutral HMS derivatives are smaller (≤17 nm) than those of the corresponding ionic MCM-41 materials (≥34 nm). The smaller particle sizes, along with defects in channel packing, result in complementary textural mesoporosity that provides for better access to the framework-confined mesopores in adsorption and catalysis by guest molecules. The textural mesopore volume in HMS molecular sieves is truly complementary and does not occur at the expense of the framework-confined mesoporosity.

**Acknowledgment.** The support of this research by the National Science Foundation through CRG Grant 92-24102 is gratefully acknowledged.

CM950549A